
MAJOR PAPER

Differences in Signal Intensity and Enhancement on MR Images of the Perivascular Spaces in the Basal Ganglia versus Those in White Matter

Shinji Naganawa^{*}, Toshiki Nakane, Hisashi Kawai, and Toshiaki Taoka

Purpose: To elucidate differences between the perivascular space (PVS) in the basal ganglia (BG) versus that found in white matter (WM) using heavily T₂-weighted FLAIR (hT₂-FL) in terms of 1) signal intensity on non-contrast enhanced images, and 2) the degree of contrast enhancement by intravenous single dose administration of gadolinium based contrast agent (IV-SD-GBCA).

Materials and Methods: Eight healthy men and 13 patients with suspected endolymphatic hydrops were included. No subjects had renal insufficiency. All subjects received IV-SD-GBCA. MR cisternography (MRC) and hT₂-FL images were obtained prior to and 4 h after IV-SD-GBCA. The signal intensity of the PVS in the BG, subsular WM, and the cerebrospinal fluid (CSF) in Ambient cistern (CSF_{AC}) and CSF in Sylvian fissure (CSF_{Syl}) was measured as well as that of the thalamus. The signal intensity ratio (SIR) was calculated by dividing the intensity by that of the thalamus. We used 5% as a threshold to determine the significance of the statistical test.

Results: In the pre-contrast scan, the SIR of the PVS in WM (Mean ± standard deviation, 1.83 ± 0.46) was significantly higher than that of the PVS in the BG (1.05 ± 0.154), CSF_{Syl} (1.03 ± 0.15) and the CSF_{AC} (0.97 ± 0.29). There was no significant difference between the SIR of the PVS in the BG compared to the CSF_{AC} and CSF_{Syl}. For the evaluation of the contrast enhancement effect, significant enhancement was observed in the PVS in the BG, the CSF_{AC} and the CSF_{Syl} compared to the pre-contrast scan. No significant contrast enhancement was observed in the PVS in WM.

Conclusion: The signal intensity difference between the PVS in the BG versus WM on pre-contrast images suggests that the fluid composition might be different between these PVSs. The difference in the contrast enhancement between the PVSs in the BG versus WM suggests a difference in drainage function.

Keywords: *gadolinium, glymphatic system, magnetic resonance imaging, perivascular space*

Introduction

Virchow-Robin spaces (VRSs), also known as perivascular spaces (PVSs), surround the walls of vessels as they course from the subarachnoid space through the brain parenchyma.¹ Dilated VRSs are frequently observed in three characteristic locations. Type I VRSs appear along the lenticulostriate arteries entering the basal ganglia (BG). Type II VRSs are found along the paths of the perforating medullary arteries as they move through the cortical gray matter into the white

matter. Type III VRSs appear in the midbrain.¹ In elderly patients, hyperintense lesions in the deep subcortical white matter including dilated VRSs are frequently observed on T₂-weighted MR images.² Perivascular spaces are usually believed to show visually similar signal intensity to cerebrospinal fluid (CSF) on most MR pulse sequences. However, PVSs have a slightly different signal intensity from CSF with quantitative analysis, suggesting that the content of the PVS may be interstitial fluid, not CSF.¹

In type II VRSs, subsular PVSs are quite common. The subsular T₂-bright structures are visualized typically as a featherlike configuration in 95% of subjects.³ Histological analysis shows that the subsular T₂-bright structures correspond to dilated PVSs.³ In another pathological study, the subsular T₂-bright area corresponded not only to dilated perivascular space, but also to demyelination and gliosis.⁴ It has been reported that the PVSs in the BG and in subcortical white matter (WM) differ both morphologically and

Department of Radiology, Nagoya University Graduate School of Medicine, 65 Tsurumai-cho, Shouwa-ku, Nagoya, Aichi 466-8550, Japan

*Corresponding author, Phone: +81-52-744-2327, Fax: +81-52-744-2335, E-mail: naganawa@med.nagoya-u.ac.jp

©2018 Japanese Society for Magnetic Resonance in Medicine

This work is licensed under a Creative Commons Attribution-NonCommercial-NoDerivatives International License.

Received: September 19, 2017 | Accepted: December 8, 2017

functionally.^{5,6} On high resolution MR images, the PVSs in WM lack an apparent communication with the subarachnoid space, unlike the PVSs in the BG.⁶ The number of PVS in the BG were correlated significantly with hypertension and lacunar stroke; however in WM, the number of PVS were correlated with hypertension but not with lacunar stroke.⁵ It is speculated that the PVSs in WM may reflect dilated interstitial fluid spaces as well as cerebral amyloid angiopathy.⁶

The heavily T₂-weighted 3D-fluid attenuated inversion recovery sequence (hT₂-FL) is quite sensitive to subtle alterations of fluid composition.⁷⁻⁹ This sequence permitted the visualization of contrast enhancement of the PVSs in the BG at 4 h after intravenous administration of single dose gadolinium based contrast agent (IV-SD-GBCA) in subjects with normal renal function.¹⁰

The purpose of the present study was to elucidate differences between the PVS in the BG versus that found in WM using hT₂-FL imaging in terms of 1) signal intensity on non-contrast enhanced images, and 2) the degree of contrast enhancement after IV-SD-GBCA.

Materials and Methods

Eight healthy men (ages: 29–53) and 13 patients with suspected endolymphatic hydrops (4 men, 9 women; ages: 27–74) were included in this study. All subjects received single dose IV-GBCA of 0.1 mmol/kg body weight using Gadoteridol (Gd-HP-DO3A: ProHance, Eisai Co., Ltd., Tokyo, Japan). In this study, we defined renal insufficiency as the history of proteinuria within 3 months or an estimated glomerular filtration rate (eGFR) of less than 60 mL/min/1.73 m². No subjects had renal insufficiency.

Magnetic resonance cisternography (MRC) and hT₂-FL images were obtained on a 3T scanner (Magnetom Verio, Siemens Healthcare, Erlangen, Germany) prior to and 4 h after IV-SD-GBCA. All MR scans were performed using a 32-channel array head coil and generalized autocalibrating partially parallel acquisitions (GRAPPA) (acceleration factor of 2). Echo trains for the signal readout, slice thickness, FOV, matrix size and slice position were identical in both the MRC and hT₂-FL images. The voxel size was 0.5 × 0.5 × 1.0 mm³. All sequences utilized a frequency selective fat suppression pre-pulse. Further details of the MR parameters are listed in Table 1. Pulse sequence parameters and the image evaluation method for the PVSs in the BG, thalamus for signal reference, and CSF in the ambient cistern were identical to a previous study.¹⁰

On the axial MRC parallel to the anterior commissure-posterior commissure (AC-PC) line, a ROI was drawn bilaterally in the BG, the high signal intensity area in the subinsular region, the CSF in the ambient cistern and in the Sylvian fissure as well as in the center of the thalami for signal reference. Details of the ROI placement are described as follows.

The PVSs in the BG were defined as “small, sharply delineated structures with CSF-like intensity on MRC that followed the course of the perforating arteries.” If a CSF-like

Table 1 Pulse sequence parameters

| Sequence name | Type | TR (ms) | TE (ms) | Inversion time (ms) | Flip angle (degree) | Section thickness/Gap (mm) | Pixel size (mm) | Number of slices | Echo train length | FOV (mm) | Matrix size | Number of excitations | Scan time (min:sec) |
|--|----------------------------|---------|---------|---------------------|---|----------------------------|-----------------|------------------|-------------------|-----------|-------------|-----------------------|---------------------|
| MR cisternography | SPACE with restore pulse | 4400 | 544 | NA | 90/initial 180 decrease to constant 120 | 1/0 | 0.5 × 0.5 | 104 | 173 | 165 × 196 | 324 × 384 | 1.8 | 3:13 |
| Heavily T ₂ weighted 3D-FLAIR | SPACE with inversion pulse | 9000 | 544 | 2250 | 90/initial 180 decrease to constant 120 | 1/0 | 0.5 × 0.5 | 104 | 173 | 165 × 196 | 324 × 384 | 2 | 7:21 |

FLAIR, fluid attenuated inversion recovery; SPACE, sampling perfection with application-optimized contrasts using different flip angle evolutions; NA, not applied.

signal area of 3 mm or above was found, coronal reformatting was performed to exclude the CSF containing lacunes by checking the shape.¹¹ A circular 1 cm diameter ROI for the PVS in the basal ganglia was placed according to instructions described in the previous study.¹⁰ The instruction is indicated briefly below. Some part of the image data had been utilized in the previous report.¹⁰

“Select the highest axial MRC slice that contains both the AC and PC. Draw a vertical line along the center of the interhemispheric fissure (line V). Draw a horizontal line perpendicular to line V through the AC (line H). Draw an ROI posterior to line H contacting the anterior edge of the circle. The distance between the contacting point and midline should be 25–30 mm. The ROI should be placed to cover as much PVS as possible on MRC. If the VRS is not clear on MRC, a distance of 27.5 mm should be employed.” Then, the ROIs were copied onto the hT_2 -FL image and the signal intensity of the ROI was measured.

For the measurements of the PVSs in WM, we used the subinsular region. Parallel linear T_2 -high signal structures were frequently seen, which correspond to the aggregation of short PVSs in a comb- or feather-like configuration in this region.³ The aggregation of PVSs allows signal measurement by an ROI.^{3,4} The 3 mm diameter ROIs were placed within the subinsular high signal intensity area on the MRC. It was

instructed that the position of the slice and placement of the ROI should be selected to cover as many PVSs as possible on the MRC (Fig. 1).

Circular ROIs of 1 cm diameter were placed in the bilateral thalami on the same slice as the PVSs in the BG at 1 cm lateral to the midline. The 3 mm diameter ROIs were placed within the bilateral CSF spaces of the Sylvian fissure and the ambient cistern while avoiding the vessels. Then, the ROIs were copied onto the hT_2 -FL image and the signal intensity of the ROI was measured. We chose the ambient cistern for the signal measurement of the CSF according to our previous study.¹² In the ambient cistern and Sylvian fissure, the apparent signal decrease of the CSF due to flow was not seen on MRC and a significant contrast enhancement was detected on the hT_2 -FL image in the previous study of normal volunteers.¹² The CSF signal in the Sylvian fissure was also measured, considering the distance from receiver coil. The distance from the receiver coil to the ambient cistern is larger than that to subinsular region. The difference of the distance between that from the receiver coil to the Sylvian fissure and that from the receiver coil to the subinsular region is small. One experienced neuroradiologist placed the ROIs on the MRC.

The signal intensity ratio (SIR) was defined as: $SIR = \text{signal intensity (SI) of the ROI of the PVSs or the ROI of the CSF} / \text{SI of the thalami}$. The bilateral values were averaged and

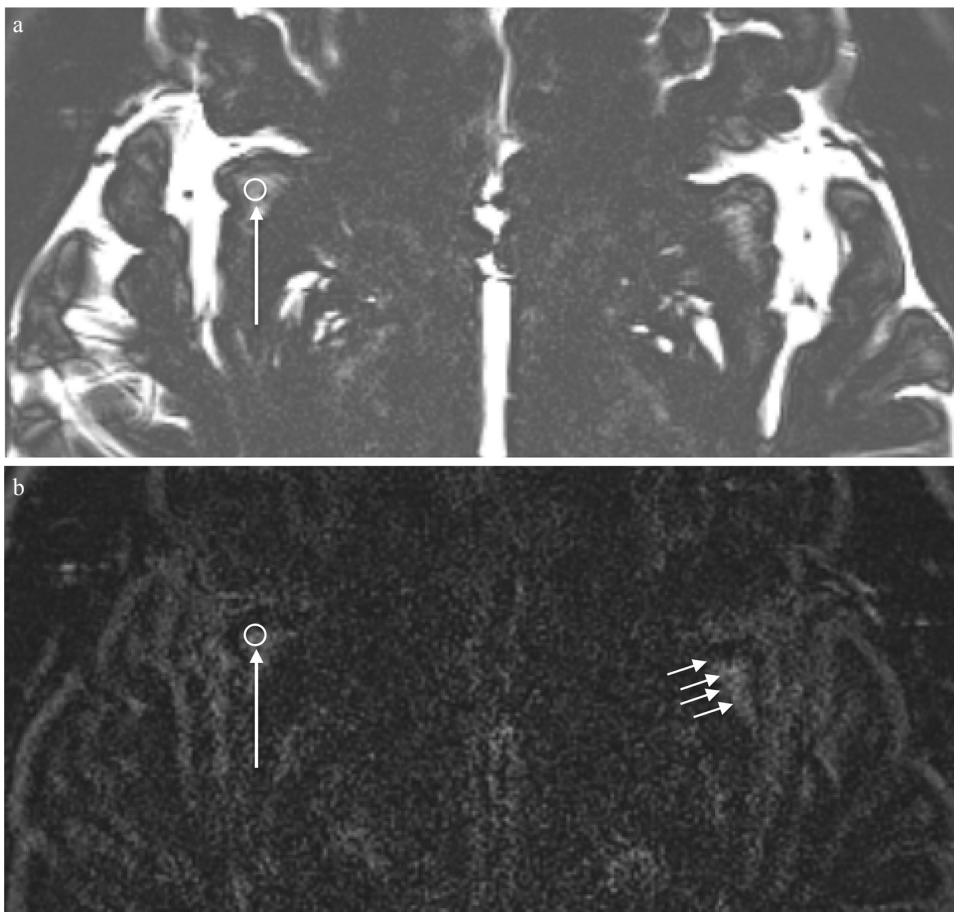


Fig. 1 A 31-year-old healthy man. An example of the ROI placement in the perivascular space of the right subinsular white matter. (a) A 3 mm circular ROI is placed to include the structures with high signal intensity in the subinsular white matter on the axial MR cisternography (MRC) image parallel to the anterior commissure-posterior commissure (AC-PC) line (arrow). This ROI is copied onto the corresponding heavily T_2 -weighted 3D-fluid attenuated inversion recovery (FLAIR) image (b) to measure the signal intensity (long arrow). Similarly, an ROI is placed on the other side and both sides were averaged for use in further analysis. (b) A corresponding heavily T_2 -weighted 3D-FLAIR image obtained prior to contrast administration. The ROI was copied from the MRC image (long arrow) to the subinsular white matter of the right side. Multiple linear or featherlike structures representing the perivascular spaces in the white matter in the corresponding left side subinsular area show high signal intensity even on this non-contrast enhanced image (short arrows).

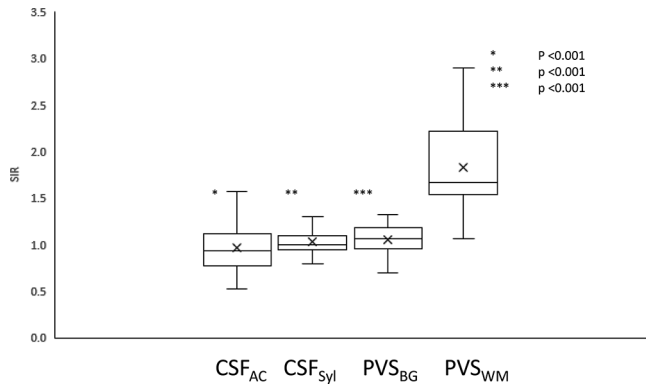


Fig. 2 The signal intensity ratio (SIR) on pre-contrast heavily T_2 -weighted 3D-fluid attenuated inversion recovery (FLAIR) images. The mean SIR of the perivascular space (PVS) in white matter (WM) is significantly higher than that in the cerebral spinal fluid (CSF) in the ambient cistern (CSF_{AC}), the CSF in the Sylvian fissure (CSF_{Syl}) and the PVS in the basal ganglia (PVS_{BG}).

used to evaluate the difference of the fluid composition in the PVS in the BG (PVS_{BG}) and the PVS in the subinsular white matter region (PVS_{WM}) compared to the CSF. We compared the pre-contrast SIR of the PVS_{BG} and PVS_{WM} , to the CSF in the ambient cistern (CSF_{AC}) and the CSF in the Sylvian fissure (CSF_{Syl}) using a univariate type III repeated-measures analysis of variance (ANOVA). A Bonferroni correction was employed for multiple comparisons. To evaluate the presence of contrast enhancement in each compartment, the SIR of the CSF_{AC} , CSF_{Syl} , PVS_{BG} , and PVS_{WM} and the signal intensity of the thalami were compared prior to, and 4 h post, IV-SD-GBCA using a paired Student's *t*-test. We used 5% as a threshold to determine the significance of the statistical test. software R (version 3.3.2, R Foundation for Statistical Computing, Vienna, Austria, <https://www.R-project.org/>) was used for the statistical analyses.

For the healthy volunteers' scans, the medical ethics committee of our institution approved the study and written informed consent was obtained from all volunteers. For the patients' retrospective study, the medical ethics committee of our institution approved this retrospective study with a waiver of written informed consent from the patients.

Results

In the pre-contrast hT_2 -FL scan, the SIR of the PVS_{WM} (Mean \pm standard deviation, 1.83 ± 0.46) was significantly higher than that of the PVS_{BG} (1.05 ± 0.15 , $P < 0.001$), the CSF_{Syl} (1.03 ± 0.15 , $P < 0.001$) and the CSF_{AC} (0.97 ± 0.29 , $P < 0.001$). There were no significant differences between the SIR of the PVS_{BG} and the CSF_{AC} , the CSF_{AC} and the CSF_{Syl} , and the PVS_{BG} and the CSF_{Syl} in the pre-contrast hT_2 -FL scan (Fig. 2).

In the evaluation of the contrast enhancement effect, there is no significant difference in the mean signal intensity of the thalami between the values on the images obtained prior to and 4 h after contrast administration ($6.20 \pm$

1.37 in pre-contrast, 5.92 ± 1.33 in post-contrast, $P = 0.224$, Fig. 3).

No significant enhancement was observed in the SIR of the PVS_{WM} (1.83 ± 0.47 in pre-contrast, 1.94 ± 0.45 in post-contrast, $P = 0.11$). The significant enhancement was observed in the PVS_{BG} (1.05 ± 0.15 in pre-contrast, 1.57 ± 0.34 in post-contrast, $P < 0.001$), CSF_{AC} (0.97 ± 0.28 in pre-contrast, 2.59 ± 0.77 in post-contrast, $P < 0.001$) and CSF_{Syl} (1.03 ± 0.15 in pre-contrast, 2.61 ± 0.78 in post-contrast, $P < 0.001$) (Fig. 3). Representative images are shown in Fig. 4.

Discussion

In the pre-contrast images of the present study, the SIR of the PVS_{WM} was significantly higher than the SIR of the CSF_{Syl} and the SIR of the PVSs in the BG. Both PVS_{WM} and PVS_{BG} showed bright signal on MRC. Therefore, the signal difference on pre-contrast hT_2 -FL images between PVS_{WM} and PVS_{BG} might be due to the difference of their T_1 values. Significant enhancement of the PVS_{WM} was not observed; however, significant enhancement of the PVS in the BG and the CSF was seen in subjects without renal insufficiency in the present study. These differences between the PVSs in the BG versus that in WM suggest two things. First, the fluid composition of the PVS_{BG} and that in the PVS_{WM} may be different. Second, the differences in contrast enhancement between the PVS_{BG} and the PVS_{WM} suggest that the drainage function within the glymphatic system of these PVSs may be different.

On routine fluid attenuated inversion recovery (FLAIR) images, it is believed that the PVS has low signal intensity.¹³ The PVS is usually seen in MR images of aged subjects; however, the PVS can be visualized in 80% of pediatric patients using routine MR images, when carefully reviewed.¹³ Histologically, the PVS is bounded by a sheet of leptomeninges, and the arterial wall in the cortical and subcortical areas. In the BG, two layers of leptomeninges cover the PVS and separate it from the subpial space.¹⁴ This histological difference between the PVS_{BG} and the PVS_{WM} might be the basis for the difference in image appearance in the present study.

The functions of the PVS are believed to be multiple, including solute distribution and waste clearance in the brain. The PVSs are routes for the glymphatic or CSF-interstitial pathway.^{15–19} Perivascular localization of aquaporin-4 (AQP4) facilitates the clearance of interstitial solutes, including amyloid-beta, through a brain-wide network of perivascular pathways termed the glymphatic system, which may be compromised in the aging brain.²⁰ Another function of the PVS is as part of the neuroimmune system. In the post-capillary PVSs, macrophages and T-cells reside as the part of blood–brain barrier (BBB) and help to modulate neuroinflammatory responses.¹⁴

Gadolinium deposition in the brain is an important issue in the medical community.^{21,22} The glymphatic system is speculated as a route for gadolinium penetration into the brain.^{10,23,24} Therefore, a better understanding of the function of PVSs is

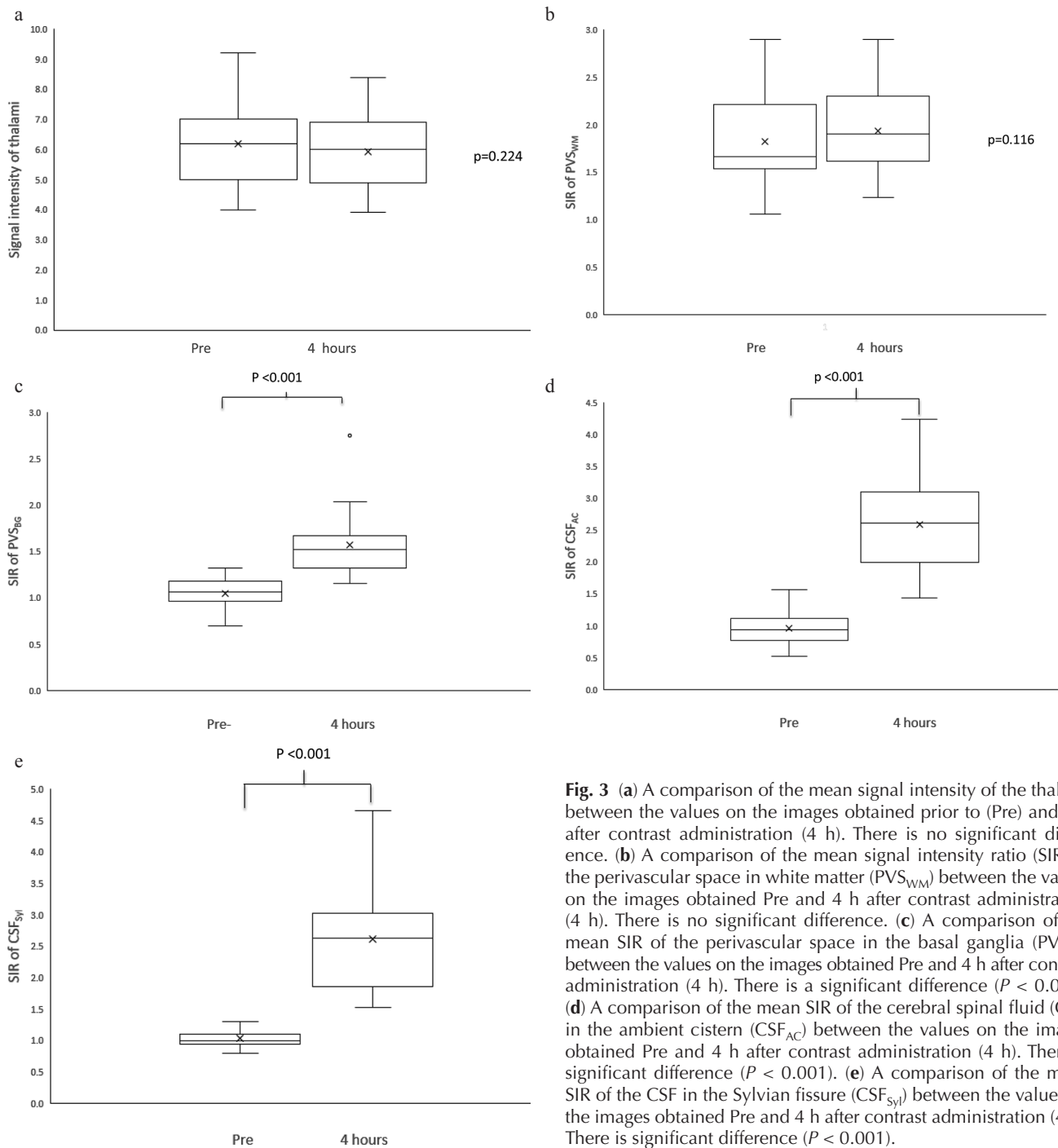


Fig. 3 (a) A comparison of the mean signal intensity of the thalami between the values on the images obtained prior to (Pre) and 4 h after contrast administration (4 h). There is no significant difference. (b) A comparison of the mean signal intensity ratio (SIR) of the perivascular space in white matter (PVS_{WM}) between the values on the images obtained Pre and 4 h after contrast administration (4 h). There is no significant difference. (c) A comparison of the mean SIR of the perivascular space in the basal ganglia (PVS_{BG}) between the values on the images obtained Pre and 4 h after contrast administration (4 h). There is a significant difference ($P < 0.001$). (d) A comparison of the mean SIR of the cerebral spinal fluid (CSF) in the ambient cistern (CSF_{AC}) between the values on the images obtained Pre and 4 h after contrast administration (4 h). There is significant difference ($P < 0.001$). (e) A comparison of the mean SIR of the CSF in the Sylvian fissure (CSF_{Syl}) between the values on the images obtained Pre and 4 h after contrast administration (4 h). There is significant difference ($P < 0.001$).

quite important, not only for general neuroscience research, but also to address specifically the issue of gadolinium deposition in the brain. There are multiple reports regarding differences between the PVS_{BG} and the PVS_{WM}.^{5,6} The severity of PVS dilation in the BG correlates with lacunar stroke, but that of PVS dilation in WM does not.⁵ Alternatively, the PVS_{WM} is speculated to be a marker of amyloid angiopathy,⁶ as well as an emerging marker of small vessel disease in aging and dementia.^{25,26} One histological study also reported that the PVS_{WM} is significantly associated with the severity of cerebral

amyloid angiopathy.²⁵ The PVS_{WM} is also reported to be a marker of mild traumatic brain injury and is suggested to be a marker of neuroinflammation.²⁷

The size of the PVS is also a cause of the differences observed on MR images. Contrast enhancement on the delayed hT₂-FL images has been reported in the PVSs of the BG.^{10,24} However, a lack of enhancement of the extremely large PVS in the BG using the same technique has also been reported.²⁸ Scan timing after IV-SD-GBCA might be a future topic of research for the visualization of enhancement in the

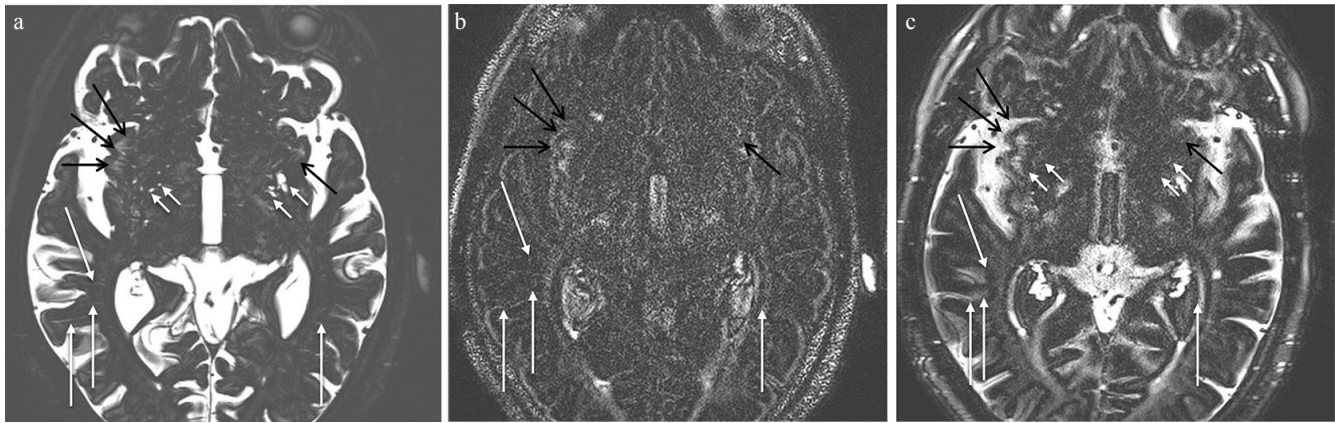


Fig. 4 A 75-year old man with suspicion of endolymphatic hydrops. (a) Magnetic resonance cisternography indicates feather-like high signal intensity in the bilateral subinsular area, corresponding to the perivascular space (PVS) in white matter (WM) (black arrows). Dilated PVS in the basal ganglia (BG) can also be seen (short arrows). Sparsely distributed long PVSs in WM other than in the subinsular area are also visualized (arrows). (b) A heavily T_2 -weighted 3D-fluid attenuated inversion recovery (FLAIR) image obtained prior to contrast administration. Although the PVSs in the subinsular WM show high signal intensity (black arrows), the PVSs in the BG do not. Sparsely distributed long PVSs in WM other than the subinsular area are also visualized as high signal intensity (arrows). (c) A heavily T_2 -weighted 3D-FLAIR image obtained 4 h after contrast administration. The PVSs in the BG show apparent enhancement (short arrows). The CSF in the bilateral Sylvian fissures and other sulci is enhanced. Sparsely distributed long PVSs in WM other than in the subinsular area are also visualized as high signal intensity (arrows). The effect of contrast enhancement is not conspicuous in these long PVSs in WM as well as the PVSs in the subinsular WM (black arrows). The signal measurement of sparsely distributed long PVS is difficult due to their small diameter.

various PVSs. Scans acquired at times other than 4 h after IV-SD-GBCA might reveal enhancement of the PVS_{WM} and the giant PVS in the basal ganglia.

It has been reported that the enhancement of the PVS_{BG} was inversely correlated with the volume of endolymphatic hydrops in the cochlea, but the volume of the PVS_{BG} was not.²⁴ Further study is warranted to reveal the relationship between the PVS_{WM} and endolymphatic hydrops.

There are some limitations to the present study. First, we included only a small number of subjects, and used manually placed small ROIs, although the ROIs were drawn according to carefully detailed guidelines. Second, the ROIs for the PVS_{WM} might have included some gliosis around the PVS. Although care was taken to avoid this contamination, it might have caused an increase in the signal intensity of the ROI on the hT_2 -FL images. We always confirmed visually that the structures with higher signal intensity that corresponded to the PVS_{WM} occupied the majority of the ROI for the PVS_{WM} on MRC and on the pre-contrast hT_2 -FL images. There is no direct contact with CSF in the subinsular WM area. There is the insular cortex between the subinsular WM area and CSF in Sylvian fissure. Therefore, the effect of CSF on the signal intensity values of PVS_{WM} might be small. Third, the ROI for the PVS_{BG} included surrounding low signal brain parenchyma. Therefore, the partial volume effect from the brain parenchyma might have influenced the signal intensity values of the ROI for PVS_{BG} . However, we have not visually noticed any higher signal of PVSs in BG compared to brain parenchyma on the pre-contrast hT_2 -FL images, thus the partial volume effect from the brain parenchyma on the signal intensity values of PVS_{BG} in the pre-contrast hT_2 -FL

images might be small. Last, we only evaluated the subinsular area of the PVS_{WM} . There are some linearly visualized PVSs in other WM areas, but their distribution is sparse and a consistent signal intensity measurement would be very difficult due to their small diameter (Fig. 4). However, the high signal intensity in the subinsular area is consistently observed even in younger subjects on the pre-contrast hT_2 -FL images.

Conclusions

The signal intensity difference between the PVS_{BG} and the PVS_{WM} on pre-contrast hT_2 -FL images suggests that the fluid composition of these PVSs might be different. The difference in contrast enhancement between the PVS_{BG} and the PVS_{WM} suggests a difference in their drainage functions within the glymphatic system of the brain. Further study is warranted to investigate the potential for the signal intensity of the PVS_{WM} on hT_2 -FL imaging as a new imaging biomarker for the evaluation of various neurological disorders.

Conflicts of Interest

The authors declare that they have no conflicts of interest.

References

1. Kwee RM, Kwee TC. Virchow-Robin spaces at MR imaging. *Radiographics* 2007; 27:1071–1086.
2. Adachi M, Sato T. Characterization of the growth of deep and subcortical white matter hyperintensity on MR imaging: a retrospective cohort study. *Magn Reson Med* 2017; 16:238–244.

3. Song CJ, Kim JH, Kier EL, Bronen RA. MR imaging and histologic features of subinsular bright spots on T2-weighted MR images: Virchow-Robin spaces of the extreme capsule and insular cortex. *Radiology* 2000; 214:671–677.
4. Tomimoto H, Lin J, Ihara M, Ohtani R, Matsuo A, Miki Y. Subinsular vascular lesions: an analysis of 119 consecutive autopsied brains. *Eur J Neurol* 2007; 14:95–101.
5. Hurford R, Charidimou A, Fox Z, Cipolotti L, Jager R, Werring DJ. MRI-visible perivascular spaces: relationship to cognition and small vessel disease MRI markers in ischaemic stroke and TIA. *J Neurol Neurosurg Psychiatry* 2014; 85:522–525.
6. Ishikawa M, Yamada S, Yamamoto K. Three-dimensional observation of Virchow-Robin spaces in the basal ganglia and white matter and their relevance to idiopathic normal pressure hydrocephalus. *Fluids Barriers CNS* 2015; 12:15.
7. Naganawa S, Kawai H, Sone M, Nakashima T. Increased sensitivity to low concentration gadolinium contrast by optimized heavily T2-weighted 3D-FLAIR to visualize endolymphatic space. *Magn Reson Med Sci* 2010; 9:73–80.
8. Naganawa S, Kawai H, Taoka T, et al. Heavily T₂-weighted 3D-FLAIR improves the detection of cochlear lymph fluid signal abnormalities in patients with sudden sensorineural hearing loss. *Magn Reson Med Sci* 2016; 15:203–211.
9. Naganawa S, Kawai H, Taoka T, et al. Cochlear lymph fluid signal increase in patients with otosclerosis after intravenous administration of gadodiamide. *Magn Reson Med Sci* 2016; 15:308–315.
10. Naganawa S, Nakane T, Kawai H, Taoka T. Gd-based contrast enhancement of the perivascular spaces in the basal ganglia. *Magn Reson Med Sci* 2017; 16:61–65.
11. Wardlaw JM, Smith EE, Biessels GJ, et al. Standards for Reporting Vascular changes on neuroimaging (STRIVE v1). Neuroimaging standards for research into small vessel disease and its contribution to ageing and neurodegeneration. *Lancet Neurol* 2013; 12:822–838.
12. Naganawa S, Suzuki K, Yamazaki M, Sakurai Y. Serial scans in healthy volunteers following intravenous administration of gadoteridol: time course of contrast enhancement in various cranial fluid spaces. *Magn Reson Med Sci* 2014; 13:7–13.
13. Groeschel S, Chong WK, Surtees R, Hanefeld F. Virchow-Robin spaces on magnetic resonance images: normative data, their dilatation, and a review of the literature. *Neuroradiology* 2006; 48:745–754.
14. Bechmann I, Galea I, Perry VH. What is the blood-brain barrier (not)? *Trends Immunol* 2007; 28:5–11.
15. Iliff JJ, Chen MJ, Plog BA, et al. Impairment of glymphatic pathway function promotes tau pathology after traumatic brain injury. *J Neurosci* 2014; 34:16180–16193.
16. Iliff JJ, Lee H, Yu M, et al. Brain-wide pathway for waste clearance captured by contrast-enhanced MRI. *J Clin Invest* 2013; 123:1299–1309.
17. Iliff JJ, Nedergaard M. Is there a cerebral lymphatic system? *Stroke* 2013; 44:S93–S95.
18. Iliff JJ, Wang M, Zeppenfeld DM, et al. Cerebral arterial pulsation drives paravascular CSF-interstitial fluid exchange in the murine brain. *J Neurosci* 2013; 33:18190–18199.
19. Jessen NA, Munk AS, Lundgaard I, Nedergaard M. The glymphatic system: a beginner's guide. *Neurochem Res* 2015; 40:2583–2599.
20. Zeppenfeld DM, Simon M, Haswell JD, et al. Association of perivascular localization of aquaporin-4 with cognition and Alzheimer disease in aging brains. *JAMA Neurol* 2017; 74:91–99.
21. Kanda T, Fukusato T, Matsuda M, et al. Gadolinium-based contrast agent accumulates in the brain even in subjects without severe renal dysfunction: evaluation of autopsy brain specimens with inductively coupled plasma mass spectroscopy. *Radiology* 2015; 276:228–232.
22. Kanda T, Ishii K, Kawaguchi H, Kitajima K, Takenaka D. High signal intensity in the dentate nucleus and globus pallidus on unenhanced T1-weighted MR images: relationship with increasing cumulative dose of a gadolinium-based contrast material. *Radiology* 2014; 270:834–841.
23. Jost G, Frenzel T, Lohrke J, Lenhard DC, Naganawa S, Pietsch H. Penetration and distribution of gadolinium-based contrast agents into the cerebrospinal fluid in healthy rats: a potential pathway of entry into the brain tissue. *Eur Radiol* 2017; 27:2877–2885.
24. Ohashi T, Naganawa S, Katagiri T, Kuno K. Relationship between contrast enhancement of the perivascular space in the basal ganglia and endolymphatic volume ratio. *Magn Reson Med Sci* 2018; 17:67–72.
25. van Veluw SJ, Biessels GJ, Bouvy WH, et al. Cerebral amyloid angiopathy severity is linked to dilation of juxtacortical perivascular spaces. *J Cereb Blood Flow Metab* 2016; 36:576–580.
26. Yao M, Hervé D, Jouvent E, et al. Dilated perivascular spaces in small-vessel disease: a study in CADASIL. *Cerebrovasc Dis* 2014; 37:155–163.
27. Inglese M, Bomsztyk E, Gonen O, Mannon LJ, Grossman RI, Rusinek H. Dilated perivascular spaces: hallmarks of mild traumatic brain injury. *AJNR Am J Neuroradiol* 2005; 26:719–724.
28. Naganawa S, Nakane T, Kawai H, Taoka T. Lack of contrast enhancement in a giant perivascular space of the basal ganglion on delayed FLAIR images: implications for the glymphatic system. *Magn Reson Med Sci* 2017; 16:89–90.